Cerebral Cortex June 2010;20:1462-1475
doi:10.1093/cercor/bhp212
Advance Access publication October 7, 2009

Role of Late Maternal Thyroid Hormones in Cerebral Cortex Development: An Experimental Model for Human Prematurity

P. Berbel[1], D. Navarro[1], E. Ausó[1], E. Varea[1], A. E. Rodríguez[1], J. J. Ballesta[1], M. Salinas[2], E. Flores[2], C. C. Faura[1] and G. Morreale de Escobar[3,4]

[1]Instituto de Neurociencias, Universidad Miguel Hernández and Consejo Superior de Investigaciones Científicas, Sant Joan d'Alacant, 03550 Alicante, Spain, [2]Biochemistry Laboratory, Hospital Universitario Sant Joan, Sant Joan d'Alacant, 03550 Alicante, Spain Madrid, [3]Instituto de Investigaciones Biomédicas Alberto Sols, Consejo Superior de Investigaciones Científicas and Universidad Autónoma de Madrid, 28029 Madrid, Spain and [4]Center for Biomedical Research on Rare Diseases (CIBERER, U708), 28029 Madrid, Spain

Hypothyroxinemia affects 35–50% of neonates born prematurely (12% of births) and increases their risk of suffering neurodevelopmental alterations. We have developed an animal model to study the role of maternal thyroid hormones (THs) at the end of gestation on offspring's cerebral maturation. Pregnant rats were surgically thyroidectomized at embryonic day (E) 16 and infused with calcitonin and parathormone (late maternal hypothyroidism [LMH] rats). After birth, pups were nursed by normal rats. Pups born to LMH dams, thyroxine treated from E17 to postnatal day (P) 0, were also studied. In developing LMH pups, the cortical lamination was abnormal. At P40, heterotopic neurons were found in the subcortical white matter and in the hippocampal stratum oriens and alveus. The Zn-positive area of the stratum oriens of hippocampal CA3 was decreased by 41.5% showing altered mossy fibers' organization. LMH pups showed delayed learning in parallel to decreased phosphorylated cAMP response element-binding protein (pCREB) and phosphorylated extracellular signal-regulated kinase 1/2 (pERK1/2) expression in the hippocampus. Thyroxine treatment of LMH dams reverted abnormalities. In conclusion, maternal THs are still essential for normal offspring's neurodevelopment even after onset of fetal thyroid function. Our data suggest that thyroxine treatment of premature neonates should be attempted to compensate for the interruption of the maternal supply.

Keywords: CREB signaling, hippocampal mossy fibers, premature birth, schizophrenia, short-term memory, subplate maturation, Timm's staining

Introduction

The importance of the transfer of thyroid hormone (TH) from the mother to the fetus during the second half of human pregnancy has been highlighted in recent reviews (Glinoer and Delange 2000; Zoeller and Rovet 2004; Morreale de Escobar et al. 2008). This is particularly relevant for children born prematurely. It is especially so for extremely low-birth weight (ELBW) infants prematurely deprived of maternal TH, at a time when their own thyroid is not able to fully meet postnatal requirements (Ares et al. 1997; Williams et al. 2005). As a consequence, they are hypothyroxinemic during an important phase of brain development, the more so the earlier their gestational age at birth (Morreale de Escobar and Ares 1997; van Wassenaer and Kok 2004). The metabolism of TH during fetal life differs from that of the newborn, with those mechanisms predominating that maintain low serum 3,5,3′-L-triiodothyronine (T_3) levels and that enhance local generation of cerebral T_3 from thyroxine (T_4) (Kester et al. 2004; Morreale de Escobar et al. 2008).

The degree and duration of the transient hypothyroxinemia of prematurity (THOP) has been implicated causally in their frequently poor cognitive development and disabling cerebral palsy (den Ouden et al. 1996; Reuss et al. 1996). In the past few decades, preterm births have increased in number and been found to occur in 12% of all pregnancies. THOP can affect 35–50% of preterm neonates, who still show a high risk of neurodevelopmental alterations (Rovet and Simic 2008; Williams and Hume 2008). These alterations are more pronounced in ELBW infants compared with heavier preterm and term infants, suggesting a gradient effect of prematurity on outcome (O'Callaghan et al. 1995; Samara et al. 2008). In particular, ELBW children show a low cognitive and motor maturation compared with children born at full-term, and they require special education at school age (Samara et al. 2008). In addition, it has been reported that the risk of suffering schizophrenia is highly increased in ELBW infants (Jones et al. 1998; Smith et al. 2001).

Although THOP has long been considered as a condition not requiring medical treatment, some recent studies have revealed a relationship between THOP and brain ultrasound anomalies and neonatal illness (Huang et al. 2002; Simic et al. 2009). The possibility that postnatal TH treatment of THOP might ameliorate their poor developmental outcome, especially if born at <27 weeks, has received increasing attention. In premature children, not only is the maternal transfer of TH interrupted but also that of many other compounds such as glucose, which is fundamental for fetal brain development. Finding quantifiable alterations in the cerebral tissue due to maternal TH deficiency would also allow us to assess the influence of other factors such as alterations in the regulation of glycemic homeostasis, ischemia induced by respiratory deficiency, etc. that also delay brain development. In addition, as already indicated, premature children are deprived abruptly of maternal T_4 during a period of general immaturity of the hypothalamic–pituitary–thyroid axis. This causes THOP which is more intense and prolonged when more premature the birth (van Wassenaer and Kok 2008). In a recent study, it has been shown that T_4 treatment improved cognitive and psychomotor development in the subgroup of very early premature infants (<27 completed weeks at birth) (van Wassenaer et al. 2002). Likewise, in premature neonates born at ≤30 weeks, the levels of free T_4 (FT_4) and free T_3 (FT_3), measured from P0 until P14, were lower compared with those found in premature children born at >30 weeks, and their outcome was worse, as measured by their higher mortality and severity of lung disease (Biswas et al. 2002).

The aim of this paper is to study the role of maternal TH on offspring's cerebral cortex development after onset of fetal

thyroid function. The present experimental model may also help to identify the possible causes of neurobehavioral alterations found in premature infants because, as in our experimental model, they are prematurely deprived of maternal TH after onset of fetal thyroid function.

Table 1
Circulating TH in dams from the experimental groups, their reproductive performance, and the weight of their progeny at the indicated ages

	T_4 (ng/mL)	T_3 (ng/mL)	Number of pups per litter	Weight of pups at P0 (g)	Weight of pups at P40 (g)
C	29.9 ± 5.3	1.1 ± 0.2	10.5 ± 2.5	6.1 ± 0.2	273.0 ± 52.1
LMH + T_4	39.2 ± 10.1[a]	1.4 ± 0.4	10.2 ± 3.0	5.8 ± 1.7	258.8 ± 57.2
LMH	0.9 ± 0.5[b]	0.3 ± 0.1[b]	10.1 ± 2.3	5.7 ± 0.3	270.2 ± 54.9

Note: Results are mean values ± standard deviation.
[a]P <0.05 for LMH compared with C dams.
[b]P <0.05 for LMH compared with C and LMH + T_4 dams.

Table 2
Tissue and circulating TH in LMH and C pups

	At P0		At P40	
	T_4 (ng/g tissue)	T_3 (ng/g tissue)	T_4 (ng/mL)	T_3 (ng/mL)
C	0.94 ± 0.17	1.32 ± 0.07	45.8 ± 9.5	0.57 ± 0.11
LMH	0.87 ± 0.19	1.33 ± 0.11	46.1 ± 7.8	0.68 ± 0.14

Note: Results are mean values ± standard deviation.

Materials and Methods

Animals and Treatments

Wistar rats were housed in temperature-controlled (22–24 °C) animal quarters, with automatic light and darkness cycles of 14 and 10 h, respectively. All surgical interventions were under anesthesia by inhalation of 1.5–2% isoflurane (Laboratorios Dr. Esteve, S.A., Barcelona, Spain) in O_2 (0.9 L O_2/min). Perfusions were under deep anesthesia by injecting sodium pentobarbital (4–5 mg/100 g body weight; Vetoquinol, S.A., Lure, France) to isoflurane-anesthetized animals. Care of the animals, drugs administration, and surgical procedures were performed under veterinary control according to European Community guidelines and following approval by the Ethics Committee of our Institutions.

Young adult females, weighing ~250–300 g, were mated at E0. Experimental pregnant rats (late maternal hypothyroidism [LMH] group) were surgically thyroidectomized at E16 as previously described (Berbel et al. 1993). From the day of thyroidectomy until delivery (at P0), they were infused with rat 1–84 parathormone (PTH H3086; Bachem GmbH, Weil am Rhein, Germany) and rat calcitonin (CT; Bachem H3072). We infused 4 μg PTH/100 g body weight/day and 1 μg CT/100 g body weight/day according to DeLuca and Dani (2001). Both, PTH and CT were diluted in 0.1 M acetate buffer (pH 4.0) and simultaneously infused using osmotic mini-pumps with a delivering ratio of 1 μL/h/day (ALZET, model 2001; Alza Corporation, Mountain View, CA), placed under the dorsal skin (Ausó et al. 2004). In addition, they were supplemented with 0.16% Ibercal-D (Merck S.L., Barcelona, Spain), which contains vitamin D3 and calcium pidolate, resulting in a final concentration of 9.5 IU vitamin D3 and 11.8 mg calcium pidolate per 100 mL drinking water. One additional group was infused with T_4 from E17 to P0 (group LMH + T_4). The onset of T_4 infusion was delayed for 1 day after thyroidectomy, considering that its effects on circulating hormone levels were likely to be more rapid than the decrease of the

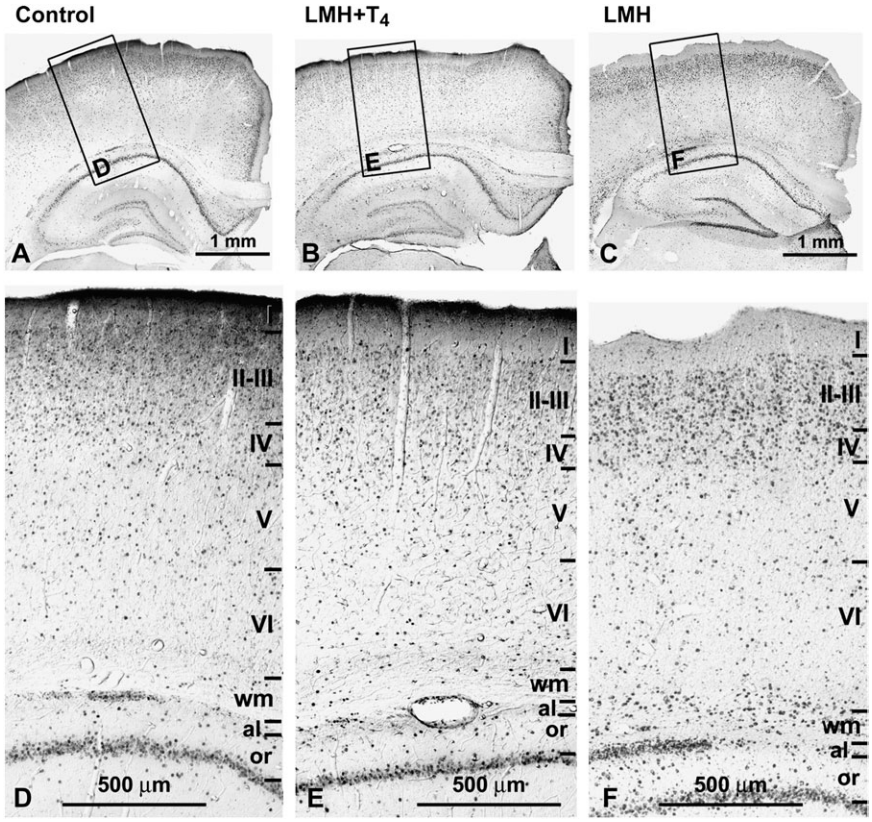

Figure 1. (*A–C*) Low-magnification photomicrographs of coronal sections of the parietal cortex and hippocampus showing BrdU-immunoreactive cells after E17–20 injections in control, LMH + T_4, and LMH pups at P40. (*D–F*) Details (boxes in *A, B,* and *C*) showing that both in layers I–VI and white matter (wm) the neocortex and the alveus (al) and stratum oriens (or) of the hippocampus, the radial distribution of BrdU-immunoreactive cells is more widespread in LMH pups than in control and LMH + T_4 pups. Note the increased number of heterotopic BrdU-immunoreactive cells in wm, al, and or in LMH pups compared with that of control and LMH + T_4 pups. The borders between layers are indicated by horizontal lines.

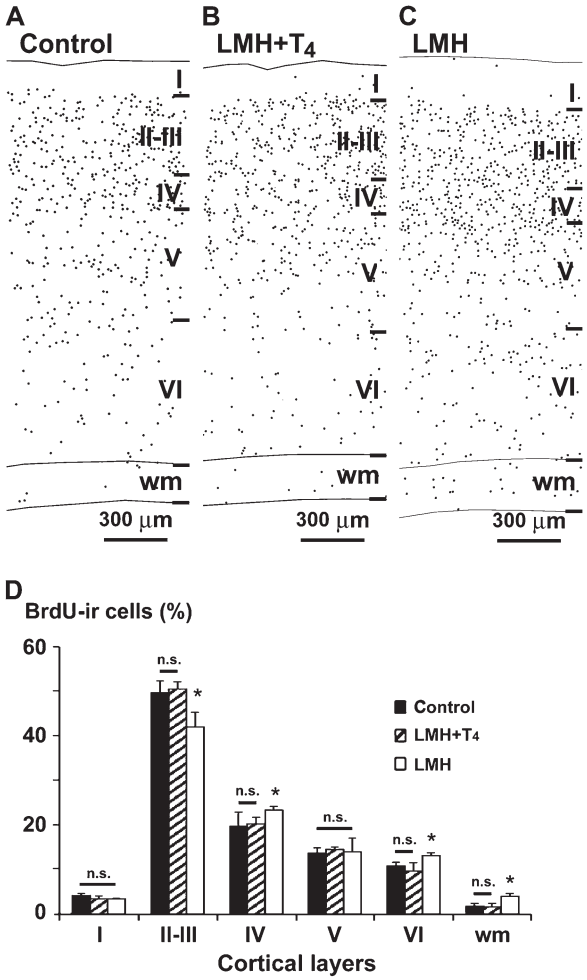

Figure 2. (*A–C*) Plots of coronal sections of the parietal cortex and hippocampus showing the distribution of type 1 and 2 BrdU-immunoreactive cells after E17–20 injections in control, LMH + T_4, and LMH pups at P40. Note the increased number of heterotopic BrdU-immunoreactive cells in the wm of LMH pups compared with that of control and LMH + T_4 pups. (*D*) Histogram showing the percentage of BrdU-immunoreactive cells in different layers of the parietal cortex in control, LMH + T_4, and LMH pups (see also Supplementary Table 3). Error bars represent ± standard deviation across layers from the same group; n.s., no significant differences; *P <0.05 for LMH group compared with C or LMH + T_4 group (n = 12 for each group).

levels caused by the thyroidectomy. We infused 2.4 μg T_4/100 g body weight/day using ALZET-2001 osmotic mini-pumps placed under the dorsal skin (Ausó et al. 2004).

At P0, LMH and LMH + T_4 pups were transferred to normal rats for lactation and nursing. These normal rats were mated on the same day as the experimental ones and on the day of delivery, their pups were sacrificed just before the transfer of the experimental pups. Control (C) pups born to sham-operated normal rats were also studied. C, LMH + T_4 and LMH dams were injected intraperitoneally once daily from E17 until P0 with 5-bromo-2-deoxyuridine (BrdU; Grupo Roche, Barcelona, Spain), 20 mg/kg body weight/day, dissolved in physiological saline.

Determination of Circulating PTH, CT, T_3, and T_4 Concentrations

Blood (~6 mL) was obtained under ether anesthesia from the heart ventricle of dams of the 3groups on the day of delivery and from their pups at P40. The plasma was spun off and kept at –20 °C, for the determination of PTH, CT, T_3, and T_4 concentrations. At P0, T_3 and T_4 levels were measured in the forebrain after their purification and extraction from the tissue as described elsewhere (Morreale de Escobar et al. 1985). The concentrations of CT were determined using a radioimmunoassay kit (Bachem S-2098) containing ^{125}I-labeled antigen and anti-CT antibody (Ab) following the procedure described in the manual. The concentrations of PTH were determined using an ELISA immunoassay kit (31-IPTRT-E01; ALPCO Diagnostics, Salem, NH) containing biotinylated anti-PTH Ab (39–84 region) for capture and horseradish peroxidase (HRP)-labeled anti-PTH Ab (1–34 region), following the procedure described in the manual. We used very sensitive and highly specific radioimmunoassays for the determination of circulating FT_4 and FT_3 concentrations (Morreale de Escobar et al. 1985).

Conventional Histology and Immunohistochemistry

Pups at P0, P8, P15, P18, P20, and P40 were weighed, anesthetized, and perfused with 50 mL of saline followed by 200 mL of 4% paraformaldehyde and 0.002% $CaCl_2$ in 10 mM phosphate buffer (PB; pH 7.3–7.4). The brains were postfixed by immersion in PB at room temperature for 4 h and stored at 4 °C in PB containing 0.5% sodium azide. Six parallel series of coronal sections of 100 μm, cut with Vibratome and containing the parietal cortex and the rostromedial portion of the hippocampal formation, were collected in phosphate buffer saline (PBS). One of these series was immunostained with anti-mature neurons neuronal nuclei (NeuN) monoclonal antibody (mAb) (1:400; Chemicon International Inc., Temecula, CA). An adjacent series was stained with cresyl violet (Sigma-Aldrich Química S.A., Madrid, Spain). At P40, 2 additional series were immunostained with anti-BrdU mAb (1:40; Amersham Pharmacia Biotech Ltd, Barcelona, Spain) and anti-vesicular Zn transporter-3 (ZnT-3) mAb (1:25), kindly provided by R. D. Palmiter (Palmiter et al. 1996). Immunolabeled sections were incubated with biotinylated horse anti-mouse Ab (1:150), Vectastain ABC kit (1:200; both from Vector Laboratories, Inc., Burlingame, CA), and 0.05% 3,3′-diaminobenzidine (DAB; Sigma-Aldrich Co., St. Louis, MO). The fifth series was double immunostained, with anti-BrdU mAb (as above), biotinylated horse anti-mouse Ab, ABC, and DAB intensified with 0.4% ammonium nickel sulfate (Ausó et al. 2001) and continued with incubation with anti-glial fibrillary acidic protein (GFAP; a marker for astrocytes) mAb (1:1000; Sigma-Aldrich Química S.A.), followed by biotinylated goat anti-rabbit Ab (1:200; Vector Laboratories, Inc.), ABC, and DAB. The sections were mounted on gelatinized slides, air dried for 24 h, dehydrated in ethanol, cleared in xylol, and coverslipped. The last series was double immunostained for fluorescence, starting with sheep anti-BrdU Ab (10 μg/mL), biotinylated rabbit anti-sheep Ab (5 μg/mL), and NeutrAvidin, Rhodamine Red conjugate (1 μg/mL; Molecular Probes Europe, Leiden, The Netherlands). It was followed with incubation with anti-NeuN mAb (1:400; Chemicon International Inc.) and then incubated with biotinylated horse anti-mouse Ab and Avidin–BODIPY FL conjugate (1 μg/mL; Molecular Probes Europe). Fluorescent sections were studied in a confocal laser fluorescence microscope.

In Situ Hybridization

Oligodendrocyte distribution was determined by in situ hybridization using proteolipid protein (PLP)/DM20 digoxigenin-labeled complementary RNA probes (PLP/DM20), kindly provided by S. Martínez (Pérez Villegas et al. 1999). Briefly, at P40, the pups were perfused for 2 min with sterile 0.1 M PBS followed by 4% paraformaldehyde in 0.1 M PBS, and brains were then postfixed overnight at 4 °C. Coronal sections at 20 μm were obtained with a cryostat. After overnight hybridization with denaturalized PLP/DM20 probes, sections were rinsed in 0.17 M saline sodium citrate buffer (pH 7.0) and incubated overnight at room temperature in alkaline phosphatase-conjugated anti-digoxigenin Ab (1/3500; Roche Diagnostics GmbH, Mannheim, Germany). The sections were then rinsed and reacted with 0.0022% 5-bromo-4-indoyl phosphate/nitroblue tetrazolium chloride (Sigma-Aldrich Co.) in 0.12 M Tris saline (pH 9.5; Sigma-Aldrich Co.). The sections were rinsed in 0.1 M PBS, dehydrated in ethanol, cleared in xylol, and coverslipped.

Ibotenic Acid Injections and Terminal Deoxynucleotidyl Transferase (TdT)-Mediated dUTP Nick-end Labeling Staining

C and LMH pups were injected with ibotenic acid at P6, P8, and P12 (3 pups per age) according to Innocenti and Berbel (1991). Anesthetized

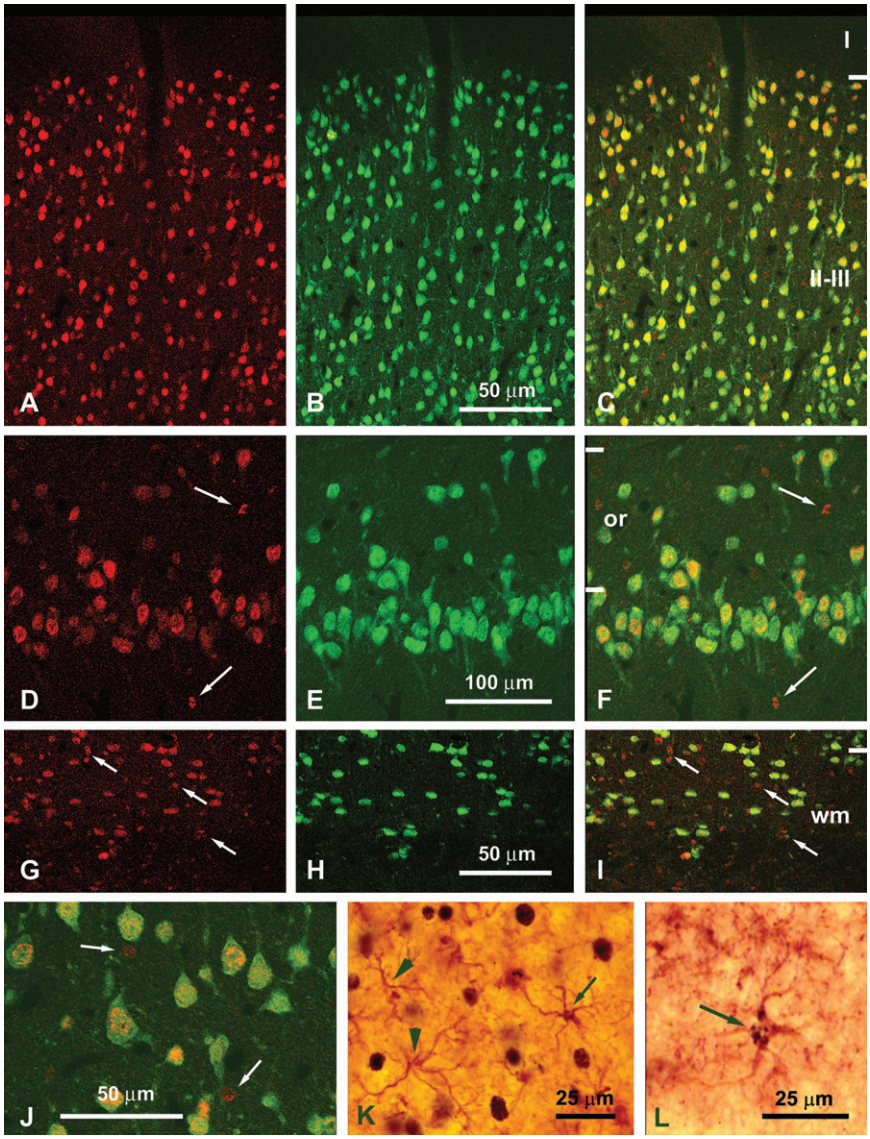

Figure 3. Confocal photomicrographs of the primary somatosensory cortex (*A–C, G–I, J*) and the hippocampal CA1 (*D–F*) of control (*J, K*) and LMH (*A–I, L*) pups at P40. Single labeling to BrdU (*A, D, G*) and to NeuN (*B, E, H*) and double labeling (*C, F, I, J*, yellow) are shown. Note that almost all BrdU-positive cells are neurons (double labeled with NeuN; *C, F, I, J*). Panels *G–I* show heterotopic neurons in the subcortical white matter (wm) of the primary somatosensory cortex in LMH pups (for comparisons between experimental groups and percentages, see Figure 6 and Supplementary Table 4). Immunofluorescence labeling of glial cells (BrdU positive and NeuN negative; arrows) in the primary somatosensory cortex of control (*J*) and LMH (*G, I*) pups. Glial cells in the hippocampal CA1 of LMH (*D, F*) pups are also indicated (arrows). Light microscope photomicrographs are shown of primary somatosensory cortex of control (*K*) and LMH (*L*) pups. Double-labeled astrocytes (arrows in *K* and *L*) are shown. Note that BrdU-labeled astrocytes show partial staining limited to clumped chromatin within the nuclei corresponding to type 3 labeling of Takahashi et al. (1992).

pups were positioned in a stereotaxic apparatus adapted for neonatal surgery (TSE Systems GmbH, Bad Homburg, Germany). After exposing the right parietal cortex, each pup received 4 injections (0.1 μL each during 5 min) of 1% ibotenic acid (Sigma-Aldrich Co.) in 0.1 M PB (pH 7.4) by a pressure picopump using glass pipettes (11–15 μm tip diameter). Injections were made at –3.6 mm from bregma and 5.0 mm lateral; the first injection was at 1000 μm depth, the second at 800 μm, the following at 600 μm, and the last at 400 μm from the surface, waiting 5 min before moving back the pipette after each injection.

After 24–26 h of survival, rats were perfused as for immunohistochemistry. Five parallel series of coronal sections of 100 μm, cut with Vibratome and containing the parietal cortex, were collected in PBS. One of these series was immunostained with anti-NeuN mAb and an adjacent series was stained with cresyl violet. One additional series was mounted on slides and processed for Terminal Deoxynucleotidyl Transferase (TdT)-Mediated dUTP Nick-end Labeling (TUNEL) according to the DeadEnd Colorimetric TUNEL kit (G7130; Promega Co., Madison, WI). Briefly, sections were incubated in proteinase K (20 μg/mL) for 15 min at room temperature and fixed again in 4% paraformaldehyde in PBS for 5 min. After washing, sections were incubated in the terminal deoxynucleotidyl transferase, recombinant reaction solution containing biotinylated nucleotides for 1 h at 37 °C, then with streptavidin-HRP, and DAB. The sections were rinsed in 0.1 M PBS, dehydrated in ethanol, cleared in xylol, and coverslipped.

Zinc Autometallography

We followed Timm's method modified by Danscher et al. (2004). At P40, 17 C, 17 LMH + T_4, and 14 LMH pups were perfused with 0.1% sodium sulfide in 0.1 M PB (pH 7.4) for 4 min. Brains were removed and frozen with liquid nitrogen. Coronal sections of 40 μm were cut with a cryostat and mounted on rinsed glass slides. Sections containing the rostromedial portion of the hippocampal formation were fixed with absolute ethanol at room temperature, rehydrated, and washed with

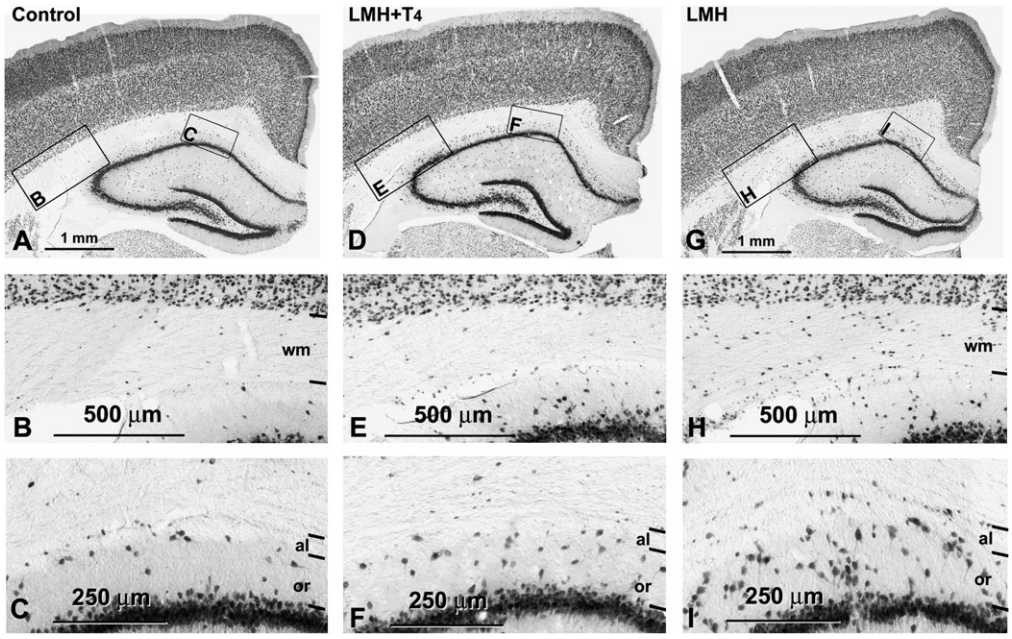

Figure 4. (*A, D, G*) Low-magnification photomicrographs of coronal sections of the parietal cortex and hippocampus showing NeuN-immunoreactive neurons in control (*A–C*), LMH + T_4 (*D–F*) and LMH (*G–I*) pups at P40. (*B, C, E, F, H, I*) Magnified boxes showing details of heterotopic NeuN-immunoreactive neurons in the subcortical white matter (wm; *B, E, H*) and in the alveus (al) and stratum oriens (or) of the hippocampus (*C, F, I*). Note the increased number of heterotopic neurons in LMH pups compared with control and LMH + T_4 pups.

distilled water. Sections were developed in 30% arabic gum, 0.86% hydroquinone and 0.11% silver lactate in 0.2 M citrate buffer, pH 4, at 26 °C for 70–75 min. Development was stopped with 5% sodium thiosulfate for 10 min and then rinsed in running tap water for 10 min. Sections were postfixed in 70% ethanol for 30 min, dehydrated in ethanol, cleared in xylol, and coverslipped.

Sodium Dodecyl Sulfate-Polyacrylamide Gel Electrophoresis and Immunoblotting

At P40, the hippocampus from 6 C and 6 LMH pups were dissected and homogenized as previously described (Valdés-Sánchez et al. 2007). Proteins (10 μg/lane) were separated on a 10% sodium dodecyl sulfate–polyacrylamide gel electrophoresis and subsequently blotted. After the transfer, nitrocellulose membranes were blocked for 1 h at room temperature with 5% dry milk in Tris-buffered saline, 0.1% Tween-20 and incubated overnight at 4 °C with the primary anti-cAMP response element-binding protein (CREB) mAb (1:1000) and anti-pCREB mAb (1:1000; both from Cell Signaling Technology, Inc., Danvers, MA), which also labels p-active transcription factor-1 (pATF1), and with anti-phosphorylated extracellular signal-regulated kinase (pERK) mAb (1:500), which also labels pERK1 and pERK2, and anti-ERK2 Ab (1:9000; both from Santa Cruz Biotechnology, Inc., Santa Cruz, CA). After incubating the secondary Ab at room temperature for 1 h, the bands were detected using ECL-Plus Western blotting detection reagents (Amersham Pharmacia Biotech Ltd, Barcelona, Spain). Finally, bands were digitalized and quantified using an LAS-1000 Bioimager (Fujifilm Co., Barcelona, Spain) and data analysis was performed using the Image Gauge 4.0 software (Fujifilm Co.). Immunolabeled nitrocellulose membranes were incubated with biotinylated horse anti-mouse Ab (1:150; Vector Laboratories, Inc.), Vectastain ABC kit (1:200; Vector Laboratories, Inc.), and 0.05% DAB (Sigma-Aldrich Co.).

Behavioral Tests

At P39, 23 C and 8 LMH pups were tested for aversive memory retrieval using a one-trial, step-down inhibitory avoidance task according to Giovannini et al. (2005). The training apparatus was a Plexiglas cage (50 × 25 × 25 cm^3) with a series of metallic bars that constituted the floor of the cage and an isolated platform (2.5 cm high, 8 cm wide, and 25 cm long) on the left end. The animals were placed on the platform facing the left rear corner of the training box. In the training session, when they stepped down putting their 4 paws on the grid, they received a 0.4-mA scrambled footshock for 2 s. After this, they were returned to their home cages. At 1 (short-term memory), 3, and 24 h (long-term memory) after training, the animals were tested again but the footshock was omitted and step-down latencies (to a ceiling of 3 min) were measured. Retention was quantified as either the step-down latency in the test session or the number of animals that did not step down during the ceiling period. After the test, they were sacrificed and processed for NeuN immunohistochemistry.

Quantification of Immunolabeled Cells and Zn-Stained Areas

We plotted only those BrdU-immunoreactive cells that showed intensely and homogenously labeled nuclei, or those that showed diffusely labeled nuclei of lesser intensity, but with clumped chromatin. These cells have entered the last S phase of their cell cycle during uptake of the injected BrdU and correspond to types 1 and 2 of Takahashi et al. (1992). For quantitative analysis of BrdU-immunoreactive cells, 2 pups from 4 litters were studied (8 pups each in C, LMH + T_4, and LMH groups) and were counted in a total of 12 probes (600 μm wide; 1–2 probes per pup). For quantitative analysis of PLP/DM20-labeled cells, we followed a similar experimental paradigm as for BrdU-immunoreactive quantification, but measurements were done in 6 probes from 3 pups each in C and LMH groups. The mean values corresponding to each pup were later used for statistical evaluation of the results. Probes were placed over the parietal cortex and spanned from layer I to the subcortical white matter, as previously detailed (Berbel et al. 2001). The borders between layers and strata were placed at the same relative depth, as measured from adjacent NeuN-immunostained sections.

For NeuN quantitative analysis, we studied 6 pups per age and group at P0, P8, P15, P20, and P40. The pups were taken from 3 litters per group. NeuN-immunoreactive cells were counted in a total of 15 probes per experimental group (2–3 probes per pup). Probes (200 μm wide) were located over the parietal cortex and spanned from layer I to the subcortical white matter. From P15 onwards, probes were located in the primary somatosensory cortex (taken at −2.0 to 4.0 mm from bregma). For each group, the relative frequencies of labeled cells in each layer were averaged across probes and animals. Plots and counts of

labeled cells were obtained using the Cellgraph system (Microptic, S.L., Barcelona, Spain).

The Zn-positive areas in the stratum oriens of CA3 were measured using the Cellgraph system in coronal sections of 17 C and 17 LMH pups taken at 2.3–2.8 mm from bregma.

Statistical Analysis

The Systat statistical software (Systat Inc., Evanston, IL) was used. For body weight, number of fetuses per litter, litter weights, concentrations of circulating hormones, Zn-positive areas in CA3, and behavioral tests, we used 1-way analysis of variance (ANOVA) and the protected least significant difference test for multiple comparisons, after validation of the homogeneity of variances by the *F* test. Frequency distributions of NeuN-immunoreactive cell density were analyzed using 2-way ANOVAs, factors being layers and experimental groups. One-way ANOVAs of immunoreactive-cell densities were followed by Tukey's test to identify significant differences ($P \leq 0.05$) between means. Data from one-trial inhibitory avoidance tests were analyzed by the Kruskal–Wallis test followed by Dunn's post hoc comparisons or chi-square test.

Results

One of the difficulties encountered during the development of the experimental model was the alteration in–calcium homeostasis caused by the thyroidectomy. Despite inserting the parathyroid glands into the sternohyoideus muscle, most not-infused LMH rats died during delivery or had fewer pups than C rats (1.8 ± 0.6 pups per litter in not-infused LMH dams [$n = 6$] vs. 10.5 ± 2.5 in C dams [$n = 26$]). The infusion of CT and PTH and the oral supply of vitamin D3 and calcium pidolate prevented hypocalcemia and both the number of successful deliveries and the number of pups per litter in LMH dams increased to reach C values (Table 1). In LMH dams, circulating CT was 0.2 ± 0.1 ng/mL (0.1 ± 0.1 ng/mL in C rats) and circulating PTH was 68.9 ± 20.8 pg/mL (46.6 ± 3.5 pg/mL in C rats). LMH rats showed very low circulating FT_4 and FT_3 concentrations compared with C dams. These values increased in LMH + T_4 dams (Table 1). No statistically significant differences were found in the levels of T_3 and T_4 between LMH and C pups, either in the forebrain at P0 or in circulation at P40 (Table 2).

At P40, in C and LMH pups, the radial distribution of types 1 and 2 BrdU-immunoreactive cells in the primary somatosensory cortex (Fig. 1*A–F* and Fig. 2*A–C*) was consistent with that described previously by Bayer and Altman (1991) showing the normal "inside–out" gradient model of radial migration. In LMH pups, the proportion of BrdU-immunoreactive cells, after injections at E17 until P0, decreased in layers II–III and increased in layers IV, VI, and white matter compared with C and LMH + T_4 pups ($P < 0.05$; Fig. 2*D* and Supplementary Table 3). At P40, double BrdU- and GFAP-immunolabeled cells were very scarce both in the neocortex and hippocampus (Fig. 3*K,L*). Double-labeled GFAP-labeled astrocytes showed disperse clumped BrdU-labeled chromatin and correspond to type 3 BrdU labeling described by Takahashi et al. (1992); these nuclei were not included in our plots and counts of BrdU-labeled cells. In contrast, all type 1 and 2 BrdU-labeled cells were also immunopositive for NeuN (Fig. 3*A,J*), both in the parietal cortex (Fig. 3*A–C,G–H*) and in hippocampal CA1 (Fig. 3*D,F*). Type 3 BrdU-positive and NeuN-negative cells accounted for less than 10% of the total NeuN-positive neurons (on average, 6.7 ± 2.1%).

These changes in cortical migration apparently did not alter the laminar organization of the cortex and hippocampus in LMH rats when NeuN-immunostained sections were observed at a low magnification (Fig. 4*A–G* and Fig. 5). At P40, no statistically significant differences were found in the thickness of the cortical layers among the 3 groups. The total thickness of the parietal cortex was on average 1715 ± 75 μm in C, 1725 ± 133 μm in LMH + T_4, and 1737 ± 92 μm in LMH pups. However, at a higher magnification, the border of layer VI with the adjacent subcortical white matter was less clear in LMH pups at P40. Heterotopic neurons were observed in the subcortical white matter and in the hippocampal stratum oriens and alveus (Fig. 4*B–F*). In C and LMH + T_4 pups, the border between the subplate and adjacent layer VI is not

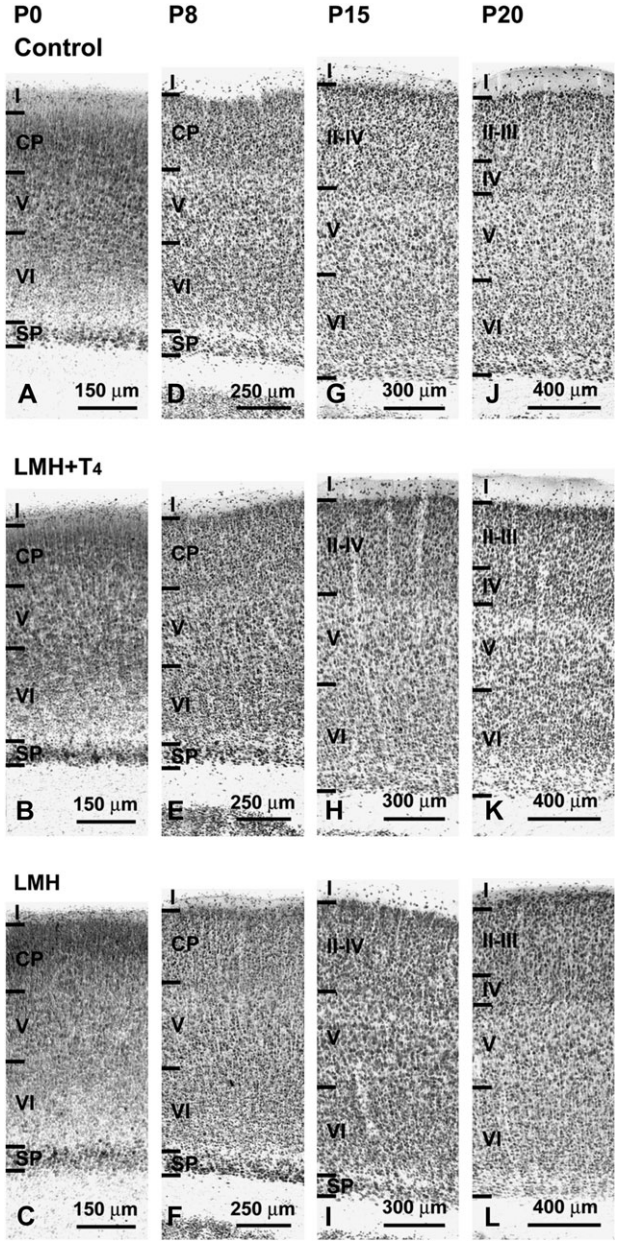

Figure 5. Photomicrographs of coronal sections of the parietal cortex showing NeuN-immunoreactive neurons in control (*A, D, G, J*), LMH + T_4 (*B, E, H, K*), and LMH (*C, F, I, L*) pups at P0, P8, P15, and P20. At P0, the subplate in LMH pups is thicker than in normal and LMH + T_4 pups (compare *C* with *A* and *B*). At P15, the border between the subplate and adjacent layer VI is more clear-cut in LMH pups (compare *I* with *G* and *H*).

distinguishable at P15 (Fig. 5*G,H* and Fig. 6*G,H*). In LMH pups, the border between the subplate and adjacent layer VI is clear-cut and the subplate contained 8.0 ± 1.9% of the total NeuN-immunoreactive neurons at this age (Fig. 5*I*, Fig. 6*I,R*, and Supplementary Table 4). In LMH pups, at P20 and P40, NeuN-immunoreactive cells decreased in layers II–III and IV and increased in layers VI and white matter compared with C and LMH + T_4 pups ($P < 0.05$; Fig. 6*J–O,S,T* and Supplementary Table 4). Using TUNEL staining, no signs of cortical cell death were observed in C and LMH pups either at P7, P9, or P13 after ibotenic acid injections at P6, P8, or P12, respectively (Fig. 7).

At P40, the radial distribution of PLP/DM20-labeled cells in the cortex and hippocampus of LMH pups was similar to that of C pups (Fig. 8*A–D*). No statically significant differences were

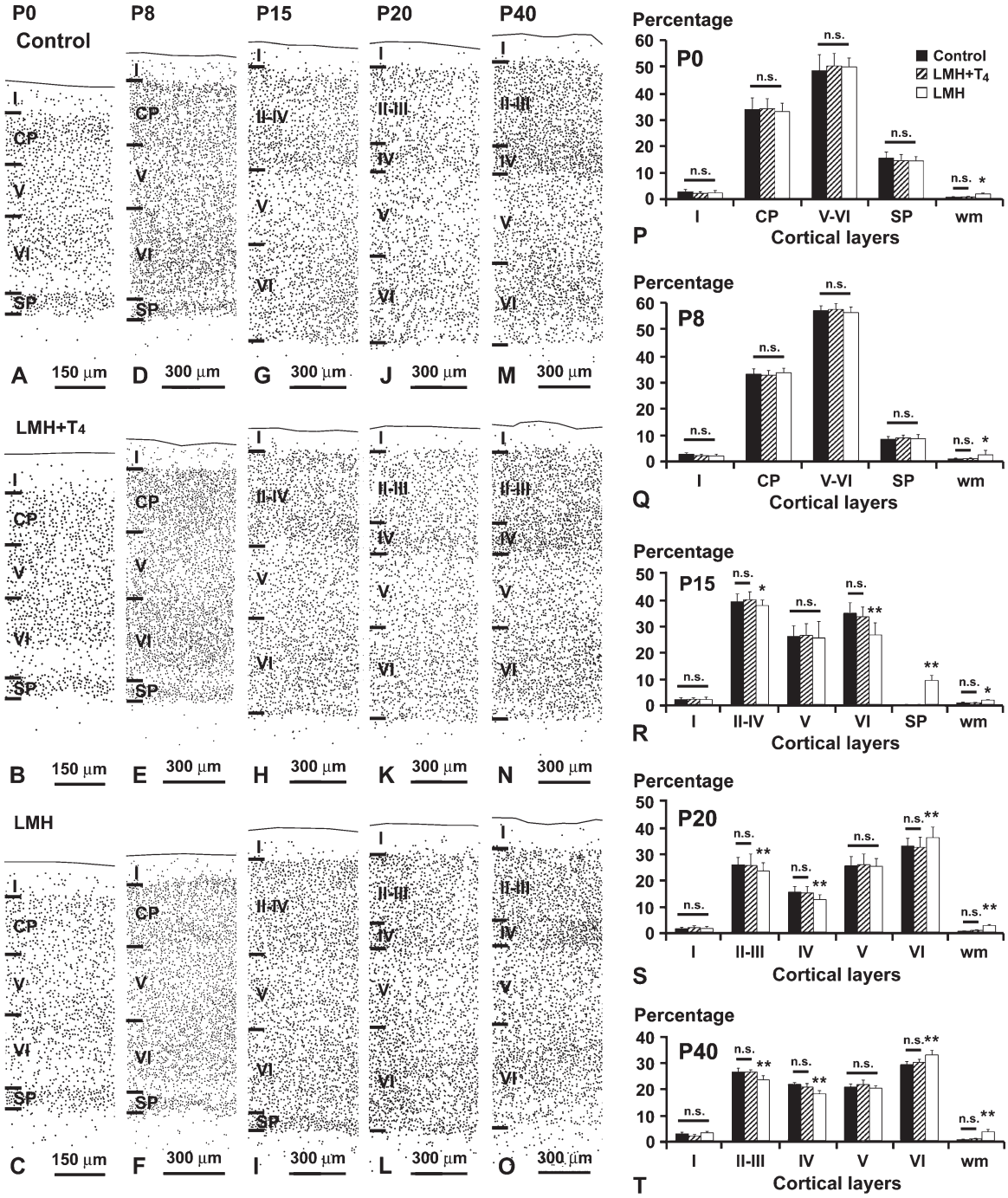

Figure 6. Plots of NeuN-immunoreactive neurons taken at similar rostrocaudal and anteroposterior of the parietal cortex in control (*A, D, G, J, M*), LMH + T_4 (*B, E, H, K, N*), and LMH (*C, F, I, L, O*) pups at P0, P8, P15, P2, and P40. At P15, the subplate is still present in LMH pups (compare *I* with *G* and *H*). (*P–T*) Histograms showing the percentage of NeuN-immunoreactive neurons in different layers of the parietal cortex in control, LMH + T_4, and LMH pups at different postnatal ages (see also Supplementary Table 4). Note the high percentage of cells in the subplate (SP) at P15 and in the white matter (wm) at all ages in LMH compared with control and LMH + T_4 pups. At P20 and P40, the percentage of NeuN-immunoreactive neurons decreased in layers II–III and IV and increased in layer VI. Error bars represent ± standard deviation across layers from the same group; n.s., no significant differences; *$P < 0.1$ and **$P < 0.05$ for LMH group compared with control or LMH + T_4 group ($n = 15$ for each group); CP, cortical plate.

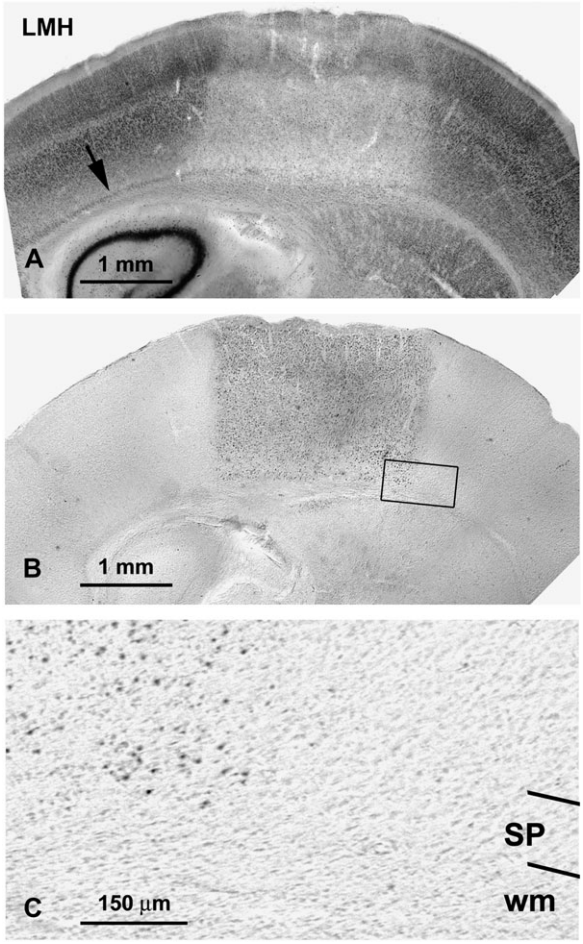

Figure 7. (*A, B*) Low-magnification photomicrographs of coronal sections of the parietal cortex showing NeuN-immunoreactive neurons (*A*) and TUNEL-labeled cells (*B*) in LMH at P13 after ibotenic acid injections at P12. Note that the zone affected by the ibotenic acid injection comprises all the cortical layers including the subplate (arrow in *A*). Photomicrograph in (*B*) is an adjacent section to (*A*) showing TUNEL-labeled cells in LMH pups. Note that the TUNEL labeling in (*B*) matches the injured area in (*A*). This box is magnified in (*C*) showing details of the subplate (SP) and subcortical white matter (wm) in the injured area (left) and in the adjacent undamaged cortex (right).

found between LMH and C rats in the percentage of labeled cells among cortical layers (Fig. 8*E*).

Zn-positive areas were observed in the cortex and hippocampal formation of C and LMH pups at P40, which coincided with previous descriptions for normal rats (Gaarskjaer 1978). As in C rats, Zn-positive areas were observed in the stratum moleculare of the dentate gyrus, the hilus of CA4, and the strata radiatum and oriens of CA3, CA2, and CA1, with increased labeling in the hilus of CA4 and in 2 bands adjacent to the pyramidal cell layer of CA3 located in the strata radiatum and oriens (Fig. 9*A–C*). However, at P40, the Zn-positive labeled area in the stratum oriens was reduced by 41.5% in LMH pups (36 464.6 ± 7972.8 μm^2) compared with C pups (64 817.7 ± 9827.0 μm^2; $P < 0.05$; Fig. 7*D–F*). ZnT-3 immunolabeling at P40 confirmed these findings, the immunolabeling in the stratum oriens of CA3 in LMH pups being much weaker than in C pups (Fig. 10*A,B*, arrowheads).

Step-down latencies were statistically lower ($P < 0.001$) in LMH (118.6 ± 19.4 s) than in C pups (158 ± 11.51 s) in the 1-h test session. The number of animals that did not step down in the ceiling period was lower ($P < 0.001$) in the LMH (one of eight) than in the C group (19 of 23), also in the 1-h test. No differences were found between the 3- and 24-h test sessions (Fig. 11). In addition, pCREB/pATF1, pCREB/CREB, pERK1/ERK2, and pERK2/ERK2 ratios in the hippocampus were reduced in LMH compared with C pups (59.1%, 66.7%, 44.4%, and 42.9%, respectively; $P < 0.001$; Fig. 12). These data indicate an altered memory consolidation in LMH pups.

Discussion

To our knowledge, this is the first study on the effects of maternal TH deficiency during the last third of gestation, without affecting the thyroid function of the fetus, on the fetal and postnatal cortical development in the progeny. In LMH pups, BrdU and NeuN immunohistochemistry showed abnormal cortical cytoarchitecture and maturation. At P15, in the parietal cortex, the border between the subplate and adjacent layer VI was still visible in LMH pups, whereas it was not in C pups, indicating abnormal cortical layering. In P40 LMH pups, heterotopic neurons were found in the subcortical white matter and stratum oriens and albeus of the hippocampus, showing altered migration during the last phase of corticogenesis. These anomalies were reverted when T_4 was infused into LMH dams. Abnormal hippocampal mossy fibers' organization was also found in LMH pups. The Zn-positive area of the stratum oriens of CA3 was decreased by 41.5% in LMH as compared with C pups. Finally, LMH pups showed delayed learning, in parallel to decreased pCREB, pERK1, and pERK2 expression in the hippocampus. Our results call attention to the importance of maternal transfer of TH after onset of fetal thyroid function. An alteration in the supply of maternal TH during the last third of pregnancy may negatively affect fetal cortical development and organization.

The Experimental Design

We have developed an animal model of late maternal hypothyroidism during pregnancy to study the offspring's neurodevelopment. In our model, we aimed to specifically affect the transfer of TH from LMH dams to fetuses one day before the beginning of fetal thyroid function (by E17.5–18) until birth (Berbel et al. 2007). To achieve this, we have thyroidectomized the dams instead of using an alternative treatment with goitrogens such as methimazole, which might also affect the thyroid function of the fetus (Morreale de Escobar et al. 1985). However, thyroidectomy presents 2 negative collateral effects. First, CT levels are depleted because the parafollicular CT-secreting cells of the thyroid are eliminated. Second, the parathyroid function is affected, even when the parathyroid glands are inserted into the sternohyoideus muscle because the short period of time between thyroidectomy and delivery is not enough for their function to recover. As a result, the death of the dams during delivery was very high (8 deaths over 10) and the number of deliveries in the successful births was dramatically reduced. It is known that PTH during fetal life may act to regulate several functions of development such as epithelial cell growth and differentiation, normal bone development and mineralization, placental calcium transport, uterine smooth muscle tone, and fetal–placental vessel tone (Wlodek et al. 2004). These functions are fundamental for normal fetal development and delivery. In addition, CT has been found to stimulate intestinal absorption

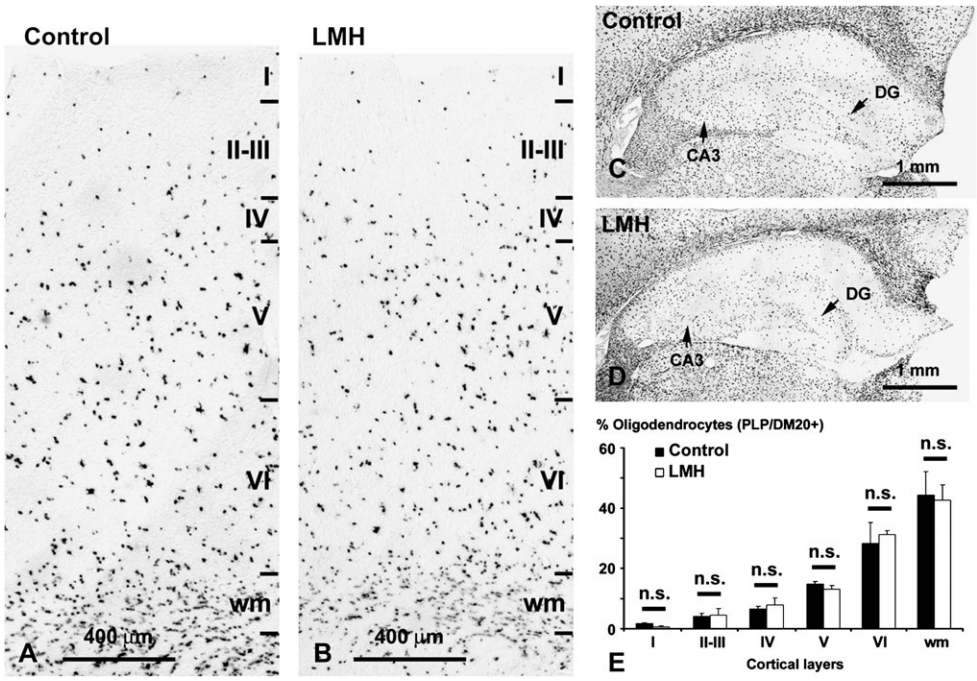

Figure 8. PLP/DM20 in situ hybridization showing the distribution of oligodendrocytes both in the parietal cortex (*A, B*) and hippocampus (*C, D*) in control and LMH pups at P40. (*E*) Histogram showing the percentages of PLP/DM20-labeled cells in control and LMH pups. No statistically significant differences (n.s.) were found between normal and LMH pups ($n = 6$ for each group) in the different layers and white matter (wm).

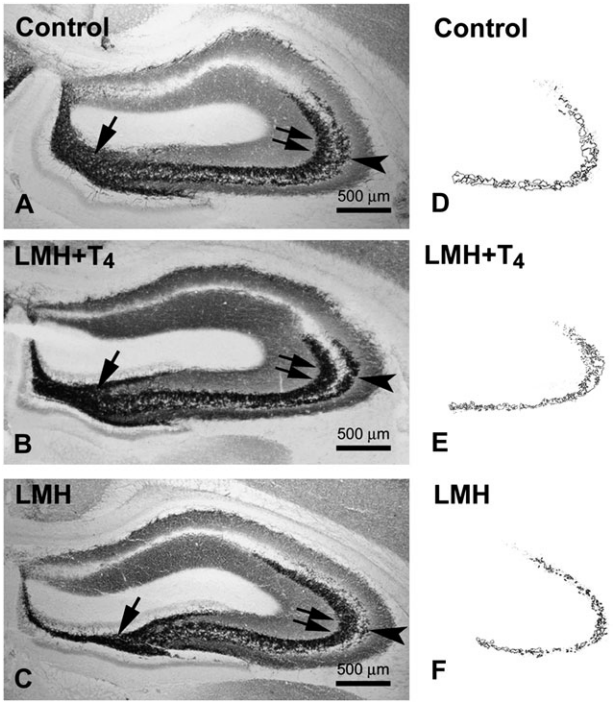

Figure 9. (*A–C*) Low-magnification photomicrographs of coronal sections of the hippocampus showing Zn labeling in control (*A, D*), LMH + T_4 (*B, E*), and LMH (*C, F*) pups at P40. Note the heavier labeling in the hilus of CA4 (arrow) and in the strata radiatum (double arrows) and oriens (arrowhead) of CA3. (*D–F*) Plots showing the Zn labeling of the stratum oriens in control, LMH + T_4, and LMH pups.

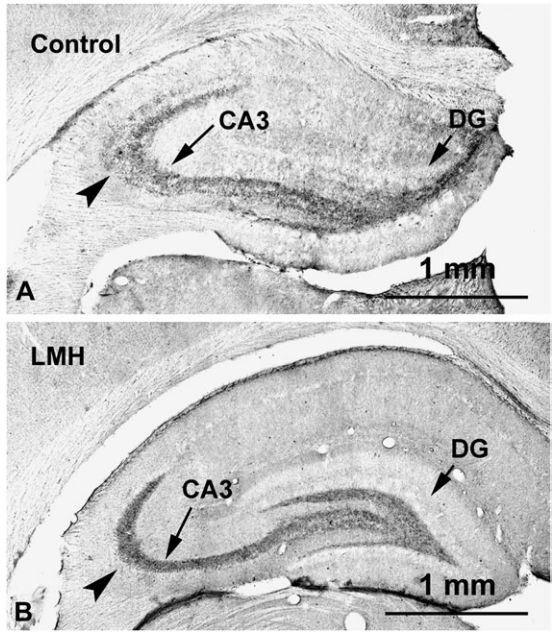

Figure 10. Photomicrographs of coronal sections of the hippocampus showing ZnT-3 labeling in control (*A*) and LMH (*B*) pups at P40. A decreased intensity of the immunolabeling can be observed in the stratum oriens (arrowhead) in LMH pups compared with controls. DG, dentate gyrus.

of calcium, by increasing circulating levels of $1,25(OH)_2D_3$ (i.e., the active form of vitamin D_3) (Jaeger et al. 1986). To overcome this situation, in the present experimental model, we have infused both CT and PTH in LMH dams. We have found that with the infusion of CT and PTH and the oral administration of vitamin D3 and calcium pidolate, the number of successful deliveries and that of the pups per litter increased in LMH dams to reach C values (Table 1). Furthermore, CT and PTH treatment of LMH dams did not alter thyroid function of LMH pups at P0 and P40 (Table 2).

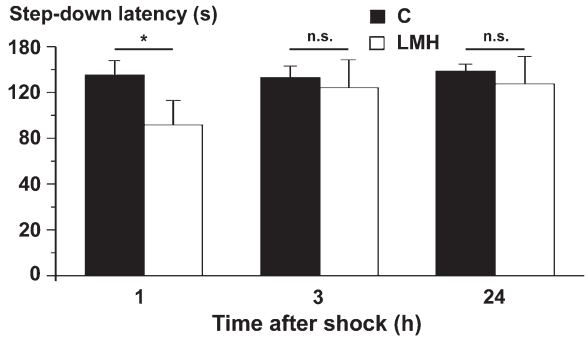

Figure 11. Histogram showing step-down latencies in seconds at 1, 3, and 24 h after the initial footshock in control and LMH pups at P39. Pups from LMH dams show a 24.9% reduction in the step-down latency at 1 h after the footshock. Error bars represent ± standard deviation; n.s., no significant differences; *P <0.001 for LMH compared with control group (n = 23 for control and n = 8 for LMH group).

The importance of using animal models both to elucidate the mechanisms of preterm parturition and to investigate possible interventions to improve outcome has been discussed recently (Elovitz and Mrinalini 2004). Current models of preterm parturition include diverse species, varying means of inducing an inflammatory or infectious state, and different routes of administration of inflammatory or infectious agents.

Several mouse genetic models of different forms of fetal and postnatal hypothyroidism, such as congenital hypothyroidism, have been described in the last decades (Kratzsch and Pulzer 2008). These models include mutations of the thyrotropin receptor ($hyt^{-/-}$ mice) (Biebermann et al. 1997), agenesis or functional impairment of thyrocytes due to thyroid transcription factor deletions ($TTF1^{-/-}$, $TTF2^{-/-}$, and $Pax8^{-/-}$ mice) (Pasca di Magliano et al. 2000), and deletions or mutations of the TH receptor ($TRa^{-/-}$, $TRb^{-/-}$, and $TRa^{-/-}b^{-/-}$ mice as well as TR*a* or TR*b* knock-in mutations) (Flamant and Samarut 2003). In these models, several combinations of maternal/fetal euthyroidism and hypothyroidism can be reached depending on the genotypes of the mother and the progeny. However, a situation in which the dam becomes hypothyroid late in pregnancy, whereas the fetus maintains a normal thyroid function, as studied here, can only be attained with our model. This is because, to the best of our knowledge, no conditional mutant mouse has yet been developed that would permit selective blocking of maternal thyroid function while preserving that of the fetus.

Despite some biological differences with respect to humans, as discussed in the review of Elovitz and Mrinalini (2004), our rat model mimics the situation of preterm neonates who must complete their neurodevelopment without a maternal TH supply. Although the postnatal development and maturation of the central nervous system is comparatively longer in humans than in rats, neocortical development occurs between the 6th and 24th week of gestation in humans and mostly before onset of fetal TH secretion that occurs at midgestation (i.e., by 18th week of gestation). In the rat, neocorticogenesis begins comparatively later, around E13 and is almost complete at birth, with most of the process occurring before E19, again mainly before onset of fetal thyroid function (at E17.5–E18), reviewed by Berbel et al. (2007). Therefore, despite the differences in timing of neurodevelopmental events between both species, similarities may be established when onset of fetal thyroid gland secretion is taken as the reference point (see Fig. 1 in Berbel et al. 2007). Our results fully support the hypothesis that neuronal migration and cortical maturation in hypothyroxinemic children could also be compromised. These alterations may well be the underlying cause of the decreased mental development described in ELBW children born prematurely (O'Callaghan et al. 1995; Kester et al. 2004; Rovet and Simic 2008; Williams and Hume 2008).

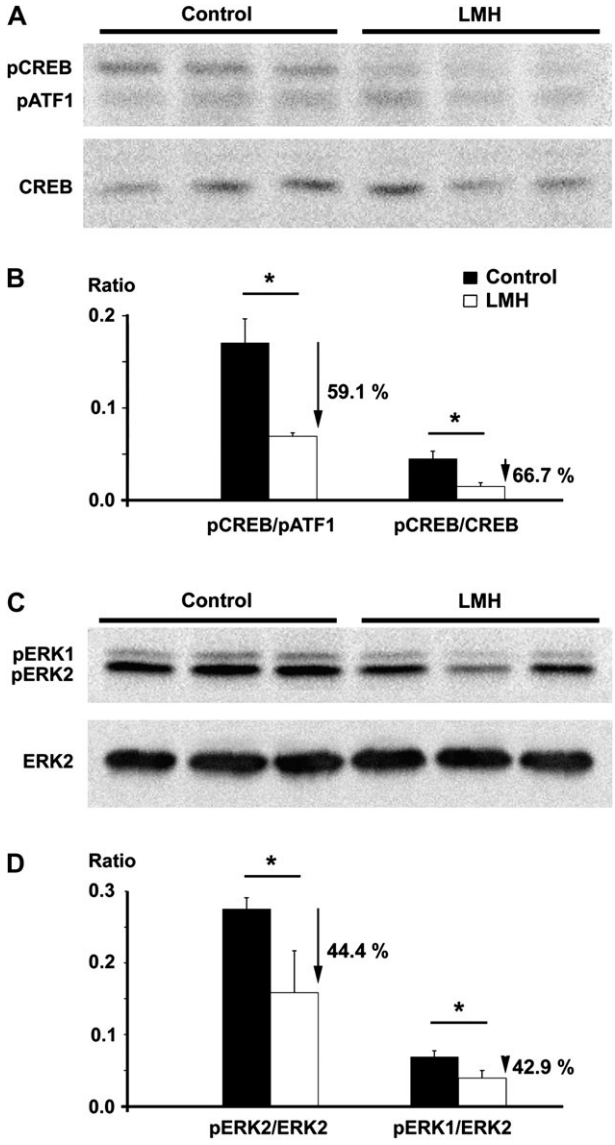

Figure 12. Western blots obtained from the hippocampus of control and LMH pups at P40, immunolabeled for pATF1, pCREB, and CREB (*A*) and ERK2, pERK1, and pERK2 (*C*). Histograms showing that the pCREB/pATF1 and pCREB/CREB (*B*) and pERK1/ERK2 and pERK2/ERK2 (*D*) ratios are reduced by 59.1%, 66.7%, 44.4%, and 42.9%, respectively, in LMH compared with control pups. Error bars represent ± standard deviation; *P <0.001 for LMH compared with control group (n = 6 for each group).

Effects on the Development and Organization of Parietal Cortex and Hippocampus

BrdU immunolabeling should be interpreted with caution because between E17 and E21, other proliferating cortical cells, such as astrocytes, might also have incorporated BrdU. Thus, BrdU labeling not only shows a pure measure of neuronal migration but also shows the position of astrocytes. However,

double-immunostained BrdU–GFAP astrocytes were very scarce compared with single GFAP-immunolabeled ones. In contrast, almost all BrdU-immunostained cells were neurons (NeuN immunopositive). The few astrocytes found that were double labeled and the type of BrdU labeling suggest that most of the astrocytes generated during the period in which the BrdU was injected died or, more likely, continued to divide postnatally, with the BrdU labeling at P40 being almost undetectable. The few BrdU-labeled astrocytes showed type 3 labeling (Takahashi et al. 1992). Thus, astrocyte labeling did not interfere with BrdU counts because only type 1 and 2 BrdU-labeled cells were plotted (see Materials and Methods). Heterotopic neurons were also found in several studies involving mild and severe TH insufficiency during gestation, indicating an abnormal radial migration of cortical neurons (Lavado-Autric et al. 2003; Ausó et al. 2004; Goodman and Gilbert 2007). However, the possibility that heterotopic neurons might also come from the medial ganglionic eminence should not be excluded. In fact, abnormal tangential migration of neurons has been found in mice born to transient and mildly hypothyroxinemic dams (Cuevas et al. 2005). The abnormalities in cell migration and the subtle changes in cytoarchitectonic organization found in LMH pups indicate that the normal process of brain maturation and, consequently, the establishment of normal brain functions are likely to be impaired.

The development and maturation of subplate neurons in rodents is not yet completely understood. Recent studies in rodents have shown that up to 50% of subplate neurons remain at P40 (Robertson et al. 2000). We have not found signs of cell death using TUNEL staining until P13; these results are in agreement with the study by Valverde et al. (1995) in the subplate of rats at different postnatal ages up to P63 leading to the conclusion that neuronal cell death does not play any significant role in the rodent subplate. These findings strongly suggest that in rodents, the subplate neurons become the adult layer VIb (Valverde et al. 1995). However, how this transition occurs is not known. In the present study, the border between the subplate and adjacent layer VI in the parietal cortex was blurred in P15 control pups, whereas it was still visible in LMH pups in similar anteroposterior and rostrocaudal levels. In addition, cortical lamination was similar in P15 LMH pups to that found in P8 control pups. Whether this altered lamination indicates a delay in the maturation of the subplate in LMH pups (e.g., caused by delay in the transition of the subplate to layer VIb) warrants further study. The use of markers for immature subplate neurons as well as for mature layer VIa and VIb neurons should clarify this point. The fate of subplate cells remains a key question to understand not only the basic mechanisms of cortical development but also the anatomical substrates of some neurological diseases. Increased persistence of interstitial white matter neurons in humans, most likely derived from subplate neurons, has been associated with several neurodevelopmental disorders such as schizophrenia and autism (Eastwood and Harrison 2003, see also below). Subplate neurons establish transient excitatory inputs to the developing cortex and converge with thalamic axons in layer IV connections (Kanold et al. 2003). These transient projections of subplate neurons to layer IV play a key role in the refinement of synaptic inputs to layer IV and may influence the outcome of ocular dominance plasticity by regulating excitatory and inhibitory inputs to layer IV (Kanold and Shatz 2006). Thus, the delay in subplate maturation may have important functional consequences not only in the organization of thalamic inputs to the neocortex but also in the maturation of cortical inhibition.

We have observed reduced mossy fibers' Zn-positive stained area in the stratum oriens of the hippocampal CA3. In agreement, reduced mossy fibers' Zn density was also found in hypothyroid pups after postnatal propylthiouracil treatment from P0 to P31 (Savage et al. 1992), as well as a decreased number of mossy fiber synapses in CA3 after propylthiouracil treatment from P0 to P30 (Madeira and Paula-Barbosa 1993). Such data suggest that reduced mossy fibers' Zn-positive stained area in the CA3 might be due to not only a decreased amount of Zn available to neurons, as the decreased ZnT-3 immunostaining suggests, but also a reduction in the number of synapses in this area. Such a reduction in the number of synapses in CA3 might explain the reduced pCREB and pERK expression that we have found in the hippocampus and the decreased step-down latency found in LMH pups. In agreement, several studies have positively correlated synaptic consolidation in the hippocampus, particularly involving mossy fibers' synaptogenesis, and memory (Bramham 2007). Performance in memory tests was indeed positively correlated with increased Timm's staining in the stratum oriens of CA3 (Ramírez-Amaya et al. 2001). Interestingly, Opazo et al. (2008) have recently found that transient maternal and fetal hypothyroxinemia in pregnant rats at the beginning of fetal corticogenesis affects spatial learning and the synaptic nature and function in the hippocampal CA1 of their offspring.

Possible Implications for Late Maternal Hypothyroidism in Man

Present results may help us to understand epidemiological findings in preterm children. The subtle changes in migration and cytoarchitectonics described here may well be the underlying cause of the decreased mental development described in children born prematurely (O'Callaghan et al. 1995; Kester et al. 2004; Rovet and Simic 2008; Williams and Hume 2008). Using image techniques such as magnetic resonance imaging (MRI; Childs et al. 1998) and diffusion tensor imaging (Skranes et al. 2007), structural abnormalities in the subcortical white matter have been reported. MRI studies observed bands of low signal intensity that were suggested to be glial cells. This was based on the fact that when the children were born most of the radial migration of the cortex is complete. However, the possibility that the tangential migration of γ-aminobutyric acidergic (GABAergic) neurons might be altered should not be ruled out. In fact, as mentioned above, gestational hypothyroxinemia affects the tangential migration of GABAergic neurons in rats (Cuevas et al. 2005).

Epidemiological studies have shown that the rate of poor fetal growth and prematurity is greater in schizophrenia than in the general population (Jones et al. 1998; Smith et al. 2001). However, the predisposition to the syndrome of schizophrenia is not yet well understood and may follow a number of distinct events mostly associated with development leading to changes in the neural circuitry, in which progressive or destructive disease events are apparently not involved (Harrison and Eastwood 2001; Lewis and Levitt 2002). In the human frontal cortex and parahippocampal gyrus, Eastwood and Harrison (2003) observed increased density of NeuN-immunoreactive neurons in the white matter adjacent to layer VI as well as

a reduced reelin expression in these interstitial neurons in schizophrenia (Eastwood and Harrison 2006). Furthermore, altered expression of other genes such as nuclear orphan transcription factor Nur-related receptor 1 (Nurr1) (Xing et al. 2006) or Neuregulin 1 is altered in schizophrenia (Harrison and Law 2006; Addington et al. 2007). Nurr1 is a dopamine-related transcription factor which in turn is also expressed in subplate neurons during cortical development, possibly playing a key role in subplate maturation (Hoerder-Suabedissen et al. 2009), whereas Neuregulin 1 is involved in key steps of corticogenesis including cell determination, interneuron migration, myelination, receptor recruitment, and synaptic plasticity (Harrison and Law 2006). In agreement with this, loss of hippocampal volume using MRI was recently reported in childhood-onset schizophrenia (Nugent et al. 2007), and in the CA3 region of the hippocampus, a 32% reduction in the number of spines forming synapses was observed in schizophrenia (Kolomeets et al. 2005).

Interestingly, the alterations that we have found in the neocortex and hippocampus of LMH pups are in concordance with such studies. Increased heterotopic neurons in the subcortical white matter and reduced mossy fibers' projection to CA3 reflect changes in cortical circuitry, similar to that found in human schizophrenia.

In conclusion, present results suggest that during development, TH have selective and permanent effects on processes that take place late during fetal development, such as cell migration and connectivity, affecting the cytoarchitectonic organization of the cerebral cortex. Any situation resulting in a decreased availability of T_4 to the fetal brain is potentially adverse for neurodevelopment. In addition, our data suggest that T_4 treatment to prematurely born neonates should be reconsidered in order to compensate for the maternal TH deficiency, and thus preventing THOP.

Supplementary Material

Supplementary material can be found at: http://www.cercor.oxfordjournals.org/

Funding

Spanish MICINN Grant (PN I+D+I SAF2006-14068 and FIS 05/PI050590).

Notes

We thank Prof. M. J. Obregón for her help with the TH determinations, Prof. J. Bernal for comments, and Dr M. C. Viso for assistance in confocal microscopy. *Conflict of Interest*: None declared.

Address correspondence to Pere Berbel, PhD, Instituto de Neurociencias, Universidad Miguel Hernández-Consejo Superior de Investigaciones Científicas, Apartado de Correos 18, Sant Joan d'Alacant, 03550 Alicante, Spain. Email: pere.berbel@umh.es.

References

Addington AM, Gornick MC, Shaw P, Seal J, Gogtay N, Greenstein D, Clasen L, Coffey M, Gochman P, Long R, et al. 2007. Neuregulin 1 (8p12) and childhood-onset schizophrenia: susceptibility haplotypes for diagnosis and brain developmental trajectories. Mol Psychiatry. 12:195–205.

Ares S, Escobar-Morreale HF, Quero J, Durán S, Presas MJ, Herruzo R, Morreale de Escobar G. 1997. Neonatal hypothyroxinemia: effects of iodine intake and premature birth. J Clin Endocrinol Metab. 82:1704–1712.

Ausó E, Cases O, Fouquet C, Camacho M, García-Velasco JV, Gaspar P, Berbel P. 2001. Protracted expression of serotonin transporter and altered thalamocortical projections in the barrelfield of hypothyroid rats. Eur J Neurosci. 14:1968–1980.

Ausó E, Lavado-Autric R, Cuevas E, Escobar del Rey F, Morreale de Escobar G, Berbel P. 2004. A moderate and transient deficiency of maternal thyroid function at the beginning of fetal neocorticogenesis alters neuronal migration. Endocrinology. 145:4037–4047.

Bayer SA, Altman J. 1991. Neocortical development. New York: Raven Press p. 255.

Berbel P, Ausó E, Garcia-Velasco JV, Molina ML, Camacho M. 2001. Role of thyroid hormones in the maturation and organisation of rat barrel cortex. Neuroscience. 107:383–394.

Berbel P, Guadaño-Ferraz A, Martínez M, Quiles JA, Balboa R, Innocenti GM. 1993. Organization of auditory callosal connections in hypothyroid rats. Eur J Neurosci. 5:1465–1478.

Berbel P, Obregón MJ, Bernal J, Escobar del Rey F, Morreale de Escobar G. 2007. Iodine supplementation during pregnancy: a public health challenge. Trends Endocrinol Metab. 18:338–343.

Biebermann H, Grüters A, Schöneberg T, Gudermann T. 1997. Congenital hypothyroidism caused by mutations in the thyrotropin-receptor gene. N Engl J Med. 336:1390–1391.

Biswas S, Buffery J, Enoch H, Bland JM, Walters D, Markiewicz M. 2002. A longitudinal assessment of thyroid hormone concentrations in preterm infants younger than 30 weeks' gestation during the first 2 weeks of life and their relationship to outcome. Pediatrics. 109:222–227.

Bramham CR. 2007. Control of synaptic consolidation in the dentate gyrus: mechanisms, functions, and therapeutic implications. Prog Brain Res. 163:453–471.

Childs AM, Ramenghi LA, Evans DJ, Ridgeway J, Saysell M, Martinez D, Arthur R, Tanner S, Levene MI. 1998. MR features of developing periventricular white matter in preterm infants: evidence of glial cell migration. Am J Neuroradiol. 19:971–976.

Cuevas E, Ausó E, Telefont M, Morreale de Escobar G, Sotelo C, Berbel P. 2005. Transient maternal hypothyroxinemia at onset of corticogenesis alters tangential migration of medial ganglionic eminence-derived neurons. Eur J Neurosci. 22:541–551.

Danscher G, Stoltenberg M, Bruhn M, Søndergaard C, Jensen D. 2004. Immersion autometallography: histochemical in situ capturing of zinc ions in catalytic zinc-sulfur nanocrystals. J Histochem Cytochem. 52:1619–1625.

DeLuca PP, Dani BA. 2001. Skeletal effects of parathyroid hormone (1-34) in ovariectomized rats with or without concurrent administration of salmon calcitonin. AAPS Pharm Sci. 3(E27):1–7.

den Ouden AL, Kok JH, Verkerk PH, Brand R, Verloove-Vanhorick SP. 1996. The relation between neonatal thyroxine levels and neurodevelopmental outcome at age 5 and 9 years in a national cohort of very preterm and/or very low birth weight premature infants. Pediatr Res. 39:142–145.

Eastwood SL, Harrison PJ. 2003. Interstitial white matter neurons express less reelin and are abnormally distributed in schizophrenia: towards an integration of molecular and morphologic aspects of the neurodevelopmental hypothesis. Mol Psychiatry. 8:821–831.

Eastwood SL, Harrison PJ. 2006. Cellular basis of reduced cortical reelin expression in schizophrenia. Am J Psychiatry. 163:540–542.

Elovitz MA, Mrinalini C. 2004. Animal models of preterm birth. Trends Endocrinol Metab. 15:479–487.

Flamant F, Samarut J. 2003. Thyroid hormone receptors: lessons from knockout and knock-in mutant mice. Trends Endocrinol Metab. 14:85–90.

Gaarskjaer FB. 1978. Organization of the mossy fiber system of the rat studied in extended hippocampi. I. Terminal area related to number of granule and pyramidal cells. J Comp Neurol. 178:49–72.

Giovannini MG, Pazzagli M, Malmberg-Aiello P, Della Corte L, Rakovska AD, Cerbai F, Casamenti F, Pepeu G. 2005. Inhibition of acetylcholine-induced activation of extracellular regulated protein kinase prevents the encoding of an inhibitory avoidance response in the rat. Neuroscience. 136:15–32.

Glinoer D, Delange F. 2000. The potential repercussions of maternal, fetal, and neonatal hypothyroxinemia on the progeny. Thyroid. 10:871–877.

Goodman JH, Gilbert ME. 2007. Modest thyroid hormone insufficiency during development induces a cellular malformation in the corpus callosum: a model of cortical dysplasia. Endocrinology. 148:2593–2597.

Harrison PJ, Eastwood SL. 2001. Neuropathological studies of synaptic connectivity in the hippocampal formation in schizophrenia. Hippocampus. 11:508–519.

Harrison PJ, Law AJ. 2006. Neuregulin 1 and schizophrenia: genetics, gene expression, and neurobiology. Biol Psychiatry. 60:132–140.

Hoerder-Suabedissen A, Wang WZ, Lee S, Davies KE, Goffinet AM, Rakic S, Parnavelas J, Reim K, Nicolic M, Paulsen O, et al. 2009. Novel markers reveal subpopulations of subplate neurons in the murine cerebral cortex. Cereb Cortex. 19:1738–1750.

Huang CB, Chen FS, Chung MY. 2002. Transient hypothyroxinemia of prematurity is associated with abnormal cranial ultrasound and illness severity. Am J Perinatol. 19:139–147.

Innocenti GM, Berbel P. 1991. Analysis of an experimental cortical network. i) Architectonics of visual areas 17 and 18 after neonatal injections of ibotenic acid; similarities with human microgyria. J Neural Transplant Plast. 2:1–18.

Jaeger P, Jones W, Clemens TL, Hayslett JP. 1986. Evidence that calcitonin stimulates 1,25-dihydroxyvitamin D production and intestinal absorption of calcium in vivo. J Clin Invest. 78: 456–461.

Jones PB, Rantakallio P, Hartikainen AL, Isohanni M, Sipila P. 1998. Schizophrenia as a long-term outcome of pregnancy, delivery, and perinatal complications: a 28-year follow-up of the 1966 north Finland general population birth cohort. Am J Psychiatry. 155:355–364.

Kanold PO, Kara P, Reid RC, Shatz CJ. 2003. Role of subplate neurons in functional maturation of visual cortical columns. Science. 301:521–525.

Kanold PO, Shatz CJ. 2006. Subplate neurons regulate maturation of cortical inhibition and outcome of ocular dominance plasticity. Neuron. 51:627–638.

Kester MH, Martínez de Mena R, Obregón MJ, Marinkovic D, Howatson A, Visser TJ, Hume R, Morreale de Escobar G. 2004. Iodothyronine levels in the human developing brain: major regulatory roles of iodothyronine deiodinases in different areas. J Clin Endocrinol Metab. 89:3117–3128.

Kolomeets NS, Orlovskaya DD, Rachmanova VI, Uranova NA. 2005. Ultrastructural alterations in hippocampal mossy fiber synapses in schizophrenia: a postmortem morphometric study. Synapse. 57:47–55.

Kratzsch J, Pulzer F. 2008. Thyroid gland development and defects. Best Pract Res Clin Endocrinol Metab. 22:57–75.

Lavado-Autric R, Ausó E, García-Velasco JV, Arufe M, Escobar del Rey F, Berbel P, Morreale de Escobar G. 2003. Early maternal hypothyroxinemia alters histogenesis and cerebral cortex cytoarchitecture of the progeny. J Clin Invest. 111:1073–1082.

Lewis DA, Levitt P. 2002. Schizophrenia as a disorder of neurodevelopment. Annu Rev Neurosci. 25:409–432.

Madeira MD, Paula-Barbosa MM. 1993. Reorganization of mossy fiber synapses in male and female hypothyroid rats: a stereological study. J Comp Neurol. 337:334–352.

Morreale de Escobar G, Ares S. 1997. The hypothyroxinemia of prematurity. J Clin Endocrinol Metab. 82:1701–1703.

Morreale de Escobar G, Ares S, Berbel P, Obregón MJ, Escobar del Rey F. 2008. The changing role of maternal thyroid hormone in fetal brain development. Semin Perinatol. 32:380–386.

Morreale de Escobar G, Pastor R, Obregón MJ, Escobar del Rey F. 1985. Effects of maternal hypothyroidism on the weight and thyroid hormone content of rat embryonic tissues, before and after onset of fetal thyroid function. Endocrinology. 117:1890–1900.

Nugent TF, 3rd, Herman DH, Ordonez A, Greenstein D, Hayashi KM, Lenane M, Clasen L, Jung D, Toga AW, Giedd JN, et al. 2007. Dynamic mapping of hippocampal development in childhood onset schizophrenia. Schizophr Res. 90:62–70.

O'Callaghan MJ, Burns Y, Gray P, Harvey JM, Mohay HI, Rogers Y, Tudehope DI. 1995. Extremely low birth weight and control infants at 2 years corrected age: a comparison of intellectual abilities, motor performance, growth and health. Early Hum Dev. 40: 115–128.

Opazo MC, Gianini A, Pancetti F, Azkcona G, Alarcón L, Lizana R, Noches V, González PA, Marassi MP, Mora S, et al. 2008. Maternal hypothyroxinemia impairs spatial learning and synaptic nature and function in the offspring. Endocrinology. 149:5097–5106.

Palmiter RD, Cole TB, Quaife CJ, Findley SD. 1996. ZnT-3, a putative transporter of zinc into synaptic vesicles. Proc Natl Acad Sci USA. 93:14934–14939.

Pasca di Magliano M, Di Lauro R, Zannini M. 2000. Pax8 has a key role in thyroid cell differentiation. Proc Natl Acad Sci USA. 97:13144–13149.

Pérez Villegas EM, Olivier C, Spassky N, Poncet C, Cochard P, Zalc B, Thomas JL, Martínez S. 1999. Early specification of oligodendrocytes in the chick embryonic brain. Dev Biol. 216:98–113.

Ramírez-Amaya V, Balderas I, Sandoval J, Escobar ML, Bermúdez-Rattoni F. 2001. Spatial long-term memory is related to mossy fiber synaptogenesis. J Neurosci. 21:7340–7348.

Reuss L, Paneth N, Lorenz JM, Pinto-Martin J, Susser M. 1996. Transient hypothyroxinemia in preterm infants and neurodevelopment at age two. N Engl J Med. 334:821–827.

Robertson RT, Annis CM, Baratta J, Haraldson S, Ingeman J, Kageyama GH, Kimm EA, Yu J. 2000. Do subplate neurons comprise a transient population of cells in developing neocortex of rats? J Comp Neurol. 426:632–650.

Rovet J, Simic N. 2008. The role of transient hypothyroxinemia of prematurity in development of visual abilities. Semin Perinatol. 32:431–437.

Samara M, Marlow N, Wolke D. EPICure Study Group 2008. Pervasive behavior problems at 6 years of age in a total-population sample of children born at </= 25 weeks of gestation. Pediatrics. 122: 562–573.

Savage DD, Otero MA, Montano CY, Razani-Boroujerdi S, Paxton LL, Kasarskis EJ. 1992. Perinatal hypothyroidism decreases hippocampal mossy fiber zinc density in rats. Neuroendocrinology. 55:20–27.

Simic N, Asztalos EV, Rovet J. 2009. Impact of neonatal thyroid hormone insufficiency and medical morbidity on infant neurodevelopment and attention following preterm birth. Thyroid. 19:395–401.

Skranes J, Vangberg TR, Kulseng S, Indredavik MS, Evensen KA, Martinussen M, Dale AM, Haraldseth O, Brubakk AM. 2007. Clinical findings and white matter abnormalities seen on diffusion tensor imaging in adolescents with very low birth weight. Brain. 130:654–666.

Smith GN, Flynn SW, McCarthy N, Meistrich B, Ehmann TS, MacEwan GW, Altman S, Kopala LC, Honer WG. 2001. Low birth weight in schizophrenia: prematurity or poor fetal growth? Schizophr Res. 47:177–184.

Takahashi T, Nowakowski RS, Caviness JV, Jr. 1992. BUdR as an S-phase marker for quantitative studies of cytokinetic behaviour in the murine cerebral ventricular zone. J Neurocytol. 21:185–197.

Valdés-Sánchez L, Escámez T, Echevarria D, Ballesta JJ, Tabarés-Seisdedos R, Reiner O, Martínez S, Geijo-Barrientos E. 2007. Postnatal alterations of the inhibitory synaptic responses recorded from cortical pyramidal neurons in the Lis1/sLis1 mutant mouse. Mol Cell Neurosci. 35:220–229.

Valverde F, López-Mascaraque L, Santacana M, De Carlos JA. 1995. Persistence of early-generated neurons in the rodent subplate: assessment of cell death in neocortex during the early postnatal period. J Neurosci. 15:5014–5024.

van Wassenaer AG, Briët JM, van Baar A, Smit BE, Tamminga P, de Vijlder JM, Kok JH. 2002. Free thyroxine levels during the first weeks of life and neurodevelopmental outcome until the age of 5 years in very preterm infants. Pediatrics. 110:534–539.

van Wassenaer AG, Kok JH. 2004. Hypothyroxinaemia and thyroid function after preterm birth. Semin Neonatol. 9:3–11.

van Wassenaer AG, Kok JH. 2008. Trials with thyroid hormone in preterm infants: clinical and neurodevelopmental. Semin Perinatol. 32:423–430.

Williams FL, Hume R. 2008. Perinatal factors affecting thyroid hormone status in extreme preterm infants. Semin Perinatol. 32:398–402.
Williams FL, Mires GJ, Barnett C, Ogston SA, van Toor H, Visser TJ, Hume R. 2005. Transient hypothyroxinemia in preterm infants: the role of cord sera thyroid hormone levels adjusted for prenatal and intrapartum factors. J Clin Endocrinol Metab. 90:4599–4606.
Wlodek ME, Di Nicolantonio R, Westcott KT, Farrugia W, Ho PW, Moseley JM. 2004. PTH/PTHrP receptor and mid-molecule PTHrP regulation of intrauterine PTHrP: PTH/PTHrP receptor antagonism increases SHR fetal weight. Placenta. 25:53–61.
Xing G, Zhang L, Russell S, Post R. 2006. Reduction of dopamine-related transcription factors Nurr1 and NGFI-B in the prefrontal cortex in schizophrenia and bipolar disorders. Schizophr Res. 84:36–56.
Zoeller RT, Rovet J. 2004. Timing of thyroid hormone action in the developing brain: clinical observations and experimental findings. J Neuroendocrinol. 16:809–818.